Geosciences Journal
Vol. 4, No. 2, p. 73 − 88, June 2000

Geological structures and evolution of the Miocene Eoil Basin, southeastern Korea

Moon Son
Hyun-Ju Seo
In-Soo Kim

Department of Geology, Pusan National University, Pusan 609-735, Korea
(e-mail: moonson@hyowon.pusan.ac.kr; seohj@hyowon.pusan.ac.kr; insookim@hyowon.pusan.ac.kr)

ABSTRACT: The Eoil Basin is one of Miocene basins in the SE Korea developed along the East Sea. The basin is bounded on the northwestern and southeastern margins by a series of normal faults trending NE or ENE, and on the northeastern and southwestern margins by a series of dextral strike-slip faults trending NNW. Erosional truncation has well-exposed the most part of basin-fills of the Eoil Basin with conspicuous stratigraphic key markers and major structures, which enabled us to construct detailed geologic and structural maps. We collected stratigraphic and structural data to get an insight into the basin genesis. We have found that the Eoil Basin has an elongate shape and consists of a series of wedge-shaped half grabens all with NE axes: the northeastern Eoil subbasin (NE subbasin) and the southwestern Eoil subbasin (SW subbasin). Based on variations in lithofacies, thickness, and age of basin-fills, it is concluded that the two subbasins experienced different evolutional history. The NE subbasin can be further divided into two fault blocks by NE-trending intrabasinal normal faults. The two blocks in the NE subbasin also experienced different subsidence rate from each other, even though almost contemporaneous. Two types of folds are recognized in the NE subbasin: simple drag fold and transverse fold. Most of our field observations indicate that the main structures (i.e., border faults, intrabasinal faults and folds) of the Eoil Basin are syndepositional, even if some of them were at least sporadically active. The sequence of the main structural development is as follows: firstly, the northwestern border faults of the NE subbasin (possibly with the southeastern border faults of the subbasin); secondly, the intrabasinal normal faults in the NE subbasin with the intrabasinal folds; thirdly, the southeastern border faults of the SW subbasin; finally, the northwestern border faults of the SW subbasin. All structural data indicate that the direction of maximum horizontal extension is NW–SE in the study area. Based on these observations and other results of previous studies, it seems that the major strike-slip faults in the study area have acted as master faults of pull-apart basin, and that the NE-trending normal faults were generated by the NW–SE tensional stress which were induced secondarily by a NNW–SSE dextral shearing acted from early Burdigalian to 15 Ma during the opening of the East Sea. We, thus, concluded that the Eoil Basin is a kind of pull-apart basin (rhombochasm) originated by the strike-slip faulting of NNW–SSE trend acted in this time span.

Key words: Miocene Eoil Basin, basin analysis, syndepositional faulting, NW–SE extension, pull-apart basin

1. INTRODUCTION

The Miocene sedimentary basins in South Korea are the most obvious results of Tertiary tectonism. Most of them are distributed in the southeastern part of the Korean peninsula, and the distribution area is roughly bounded by the Yangsan and Ulsan faults which strike NNE and NNW, respectively. The formation and evolution of the basins have been commonly attributed to the opening of the East Sea. It has been generally accepted that the basins genesis is closely related with the dextral strike-slip motions of the Yangsan and Ulsan faults caused by N–S or NNW–SSE spreading of the East Sea (Han et al., 1987; Kim, 1992; Yoon and Chough, 1995). Recent paleomagnetic studies, however, cast doubt on the roles of the Yangsan and Ulsan faults as major strike-slip faults related to the formation of the Miocene basins (Kang et al., 1996; Son et al., 1997). This is because any anomalous declination of remanent magnetization has not been observed in the areas adjacent to both faults, while it is the case in and around the Miocene basins (Kim et al., 1986; Han, 1989; Kim and Kang, 1989; Min et al., 1994; Son et al., 1996). This indicates that our understanding of the dynamic mechanism of the basin formation is not clarified yet. Thus, for a better understanding of the basin genesis, it is required to collect more reliable field data and to make a detailed structural interpretation of the basin area.

The Eoil Basin is located in the central part of the Miocene basin province in the southeastern part of the Korean peninsula (Fig. 1). Its dimension is about 12 km in length and about 5 km in maximum width, and tends to be widened toward the East Sea. Its northwestern and southeastern margins are bounded by NE- or ENE-striking faults, and the strata within the basin dip generally toward NW (Fig. 2). It is noticeable that the basin is composed of a series of parallelogram-shaped troughs developed in NE direction. The Eoil Basin is divided into three major intrabasinal fault blocks by NNW-trending border faults and NE-trending intrabasinal faults (Figs. 1 and 2). Erosional truncation has exposed the most part of the basin-fills as well as the border and internal structures (mainly faults and folds) very well. Especially, some stratigraphic key markers (one ash fall layer and two basaltic lava flows) serve as useful chronostratigraphic units. They are exposed in each of the intrabasinal fault blocks and can be traced laterally to a long distance. They, therefore, offer an excellent opportunity to examine

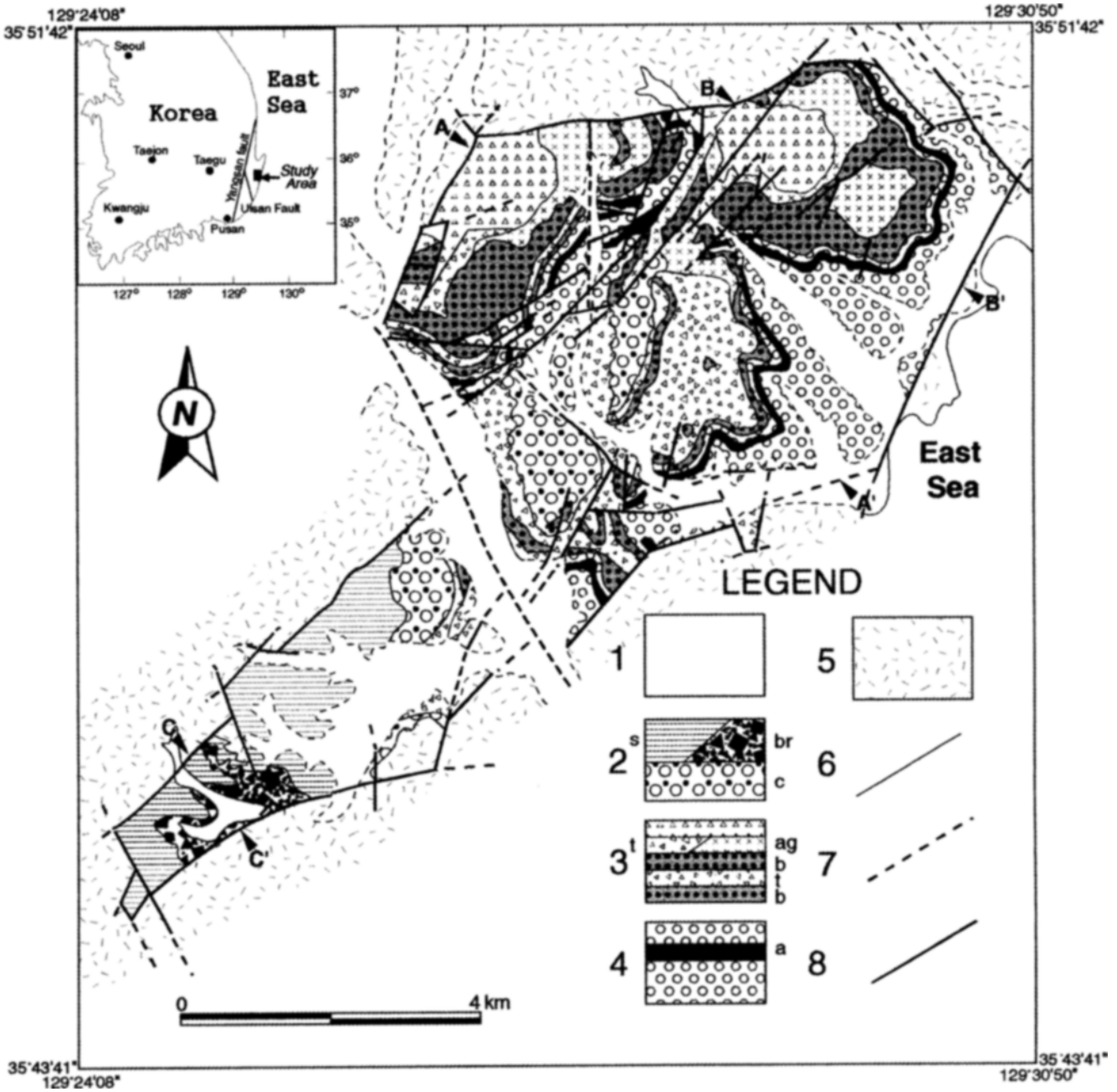

Fig. 1. Geological map of the Eoil Basin, with the locations of the cross sections in Figure 3. 1: Alluvium, 2: Songjeon Formation (s: sandstones, br: breccias, c: conglomerates), 3: Eoil Formation (l: lacustrine sedimentary rocks with tuffs, ag: agglomerates, t: tuffites, b: basaltic lavas), 4: Kampo Conglomerate (a: acidic fallout tuffs), 5: Basement rocks, 6: Geological boundary, 7. Inferred Faults, 8: Faults. Note three (a, lower b, upper b) chronostratigraphic key beds (two basaltic lavas and an acidic fallout tuffs).

how the same stratigraphic unit varies in thickness and facies depending on their structural position in the basin. They also allow to constrain the relative age of formation of the border faults, intrabasinal faults and folds.

The aim of this paper is to clarify the genesis and evolution history of the Eoil Basin. Firstly, we present the detailed geological and structural maps. They show the distributions and variations of each stratigraphic unit of the basin-fills and give the geometries of major structures, especially border fault systems and associated structures, dividing the basin into several structural domains. The relationship between structural elements and stratigraphic elements is used to infer the timings and kinematics of the major structures. Secondly, we determine the (paleo) stress fields recorded in rocks exposed in the vicinity of the border faults as well as in the basin-fills, to support our interpretation of the kinematics and dyn-

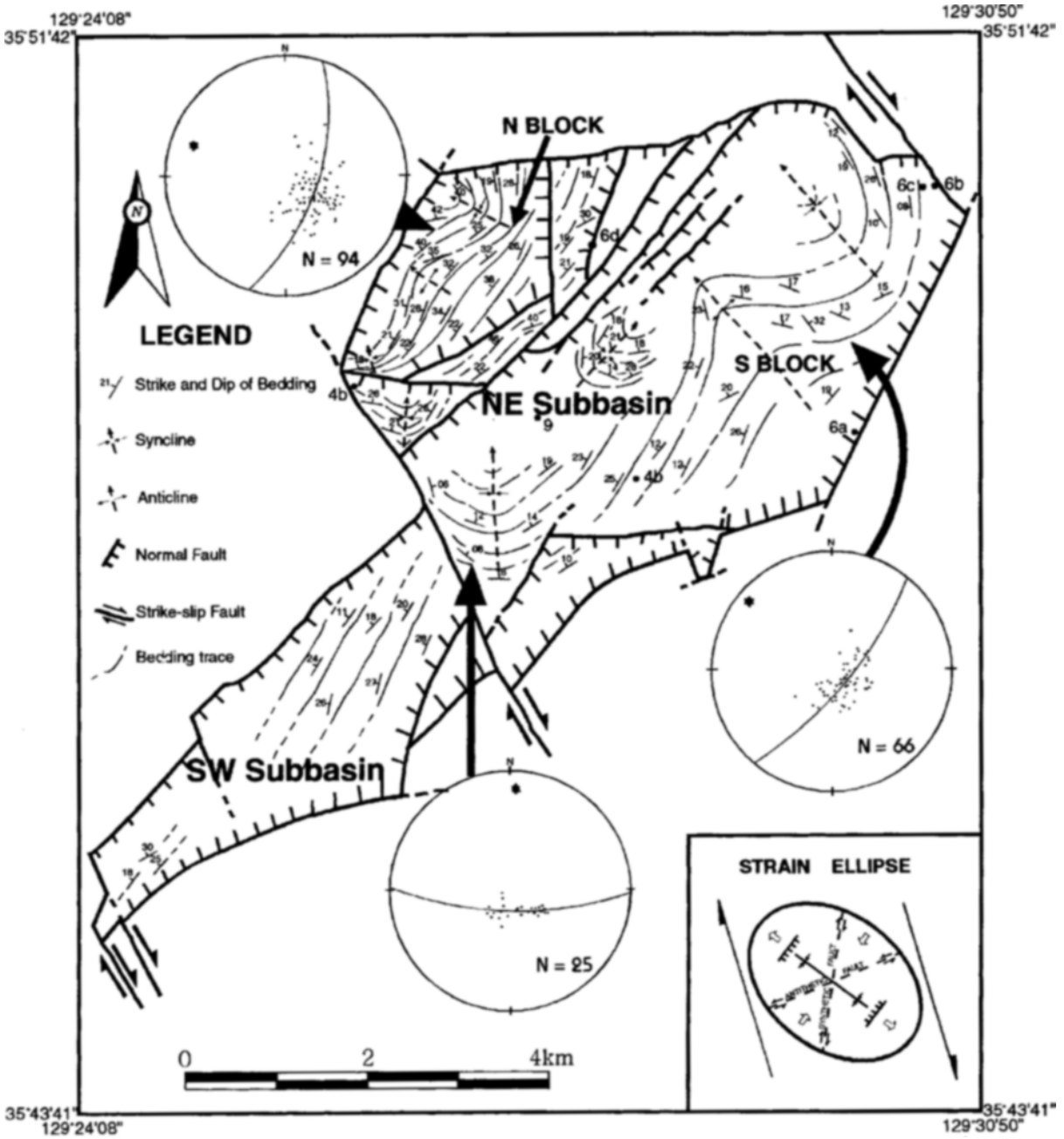

Fig. 2. Structural map of the Eoil Basin showing the traces of major faults, bedding, and fold axial-planes. Stereograms of poles to bedding with π-axis (star) of girdles. Lower-hemisphere, equal-area projection. Dots with a number represent the locations of Figures 4, 6, and 9, respectively. See the text for detailed interpretation.

amics of the border faults and the basin formation. Lastly, we examine the whole data synthetically and try to compile an evolution history of the Eoil Basin in temporal and spatial context.

2. GEOLOGICAL BACKGROUND

The name 'Eoil Basin' was first used by Kim (1970). He originally defined the basin as a series of small Tertiary basins on the east coast of the southeastern Korean Peninsula. However, Kim (1970) was not able to define the limits and geometry of his Eoil Basin because he conducted only paleontological study without detailed mapping and structural analysis. Later, it was found that the Kim's (1970) 'Eoil Basin' can be divided into three parts separated each other by basement rocks and that each part is bounded by faults (Lee et al., 1992; Son and Kim, 1994; Son, 1998). Besides, their basin-fills seem to be different in stratigraphy and litho-

facies from each other. Therefore, the southern two parts are named separately as Haseo Basin (Lee et al., 1992) and Chongja Basin (Son and Kim, 1994). This study area is the northern part of the Kim's (1970) 'Eoil Basin'. It's the main region studied by him and includes the type-locality, Eoil-ri. We, thus, redefine the 'Eoil Basin' as a fault-bounded subsidence area surrounded by basement rocks and filled by Miocene sedimentary and volcanic rocks in this study area (Figs. 1 and 2).

The basement rocks of the Eoil Basin are composed of Cretaceous sedimentary rocks, Eocene granite (Kim et al., 1995), Paleocene–Eocene acidic volcanics (Jin et al., 1988), and Early Miocene andesites and acidic tuffs (Jin et al., 1989). The Early Miocene andesites and acidic tuffs have been called the Hyodongri Volcanics and the Waupri Tuff, respectively (Tateiwa, 1924). The stratigraphic relationship between these two units and the basin-fills is still controversial (Yoon, 1982; Chwae et al., 1988; Lee et al., 1992), because they are in contact by faults. In the present study, however, the two volcanic units are regarded as basement rocks of the basin, because they are exposed only in the footwall of the normal faults bounding the basin.

In view of sedimentary environments, three stratigraphic units are recognized in the Eoil Basin: (1) fluviatile conglomerates in the lower part (called Kampo Conglomerate), (2) basaltic lavas and tuffites with partly lacustrine sediments (Lee, 1976) in the middle part (called Eoil Formation), (3) brackish water and fluviatile sandstones and conglomerates (Yun et al., 1989; Paik et al., 1992) in the upper part (called Songjeon Formation) (Fig. 1). The Kampo Conglomerate is overlain conformably by the Eoil Formation which is again overlain unconformably by the Songjeon Formation.

The Kampo Conglomerate mostly consists of clast-supported boulder conglomerates, conglomerates, and pebbly sandstones. The lithofacies tends to be finning upward, and the lateral facies variation is virtually absent. In the upper part of the Kampo Conglomerate, one pumice-rich dacitic fallout tuff layer (Fig. 4a) with a constant thickness can be traced laterally in the basin (Fig. 1).

The Eoil Formation can be divided into five mappable units (Fig. 1): (1) lower basaltic lava (Fig. 4b), (2) tuffites composed of tuffaceous conglomerates and tuffaceous sandstones, (3) upper basaltic lava, (4) tuffaceous sandstones and agglomerates, and (5) lacustrine sedimentary rocks intercalated with tuffs (in pyroclastic terminology of Schmid, 1981). It means that the Eoil Formation was deposited initially as a basaltic lava flow and terminated as lacustrine sediments including diatomites (Lee, 1976) under the prevalent basalt-volcanic environment. The basaltic lava flows were dated as 18–20 Ma with the K–Ar whole rock method (Lee et al., 1992).

The Songjeon Formation consists of three mappable units: (1) fluviatile conglomerates in the lower part, and (2) breccias and (3) brackish water sandstones in the upper part. The breccias are intertonguing with sandstones in the southwestern part of the basin. The sandstones were dated as early Middle Miocene by molluscan fossils (Yoon, 1976).

3. VARIATIONS IN THICKNESS AND FACIES

The Eoil Basin is divided into two subbasins by a border fault striking NNW (Figs. 1 and 2): northeastern Eoil subbasin (abbreviated as NE subbasin) and southwestern Eoil subbasin (abbreviated as SW subbasin). In view of the fact that there are obvious differences in facies and ages of major constituent rocks of the two subbasins, it is considered that each subbasin has a distinct evolutional history. The NE sub-

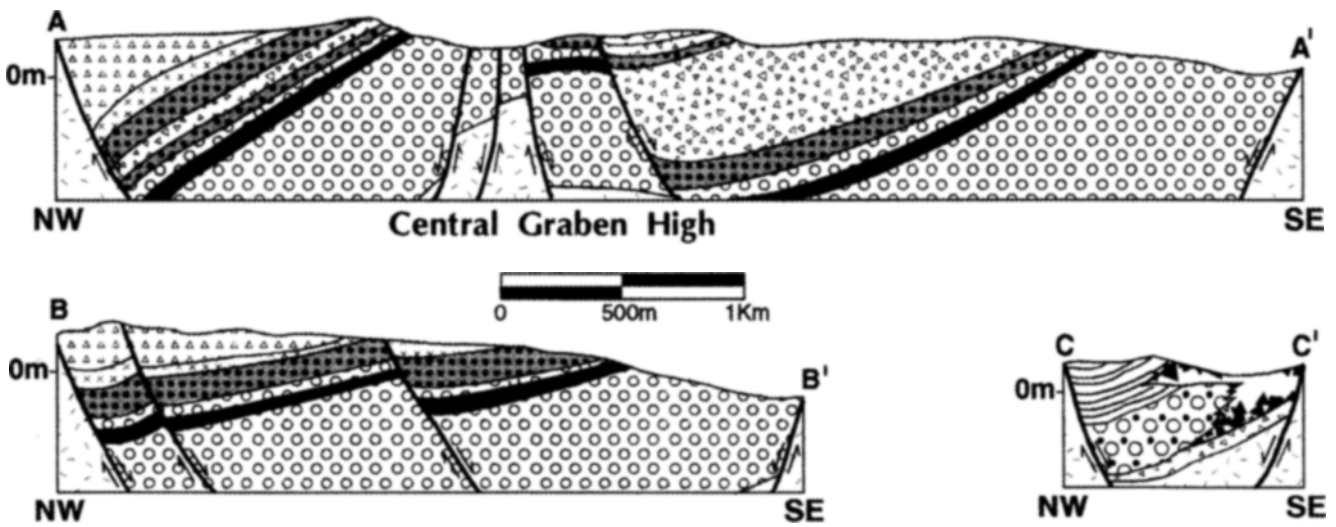

Fig. 3. Representative cross sections of the Eoil Basin, showing asymmetrical nature of the basin. See Figure 1 for the profile locations. Note the geometry of the bedding. Section A–A' shows a central graben high (terminology of Gibbs, 1984) dividing the basin into two blocks. Section C–C' shows breccias deposited in front of the southeastern border fault, which are intertonguing with conglomerates and sandstones northwestwards. No vertical exaggeration in all sections.

basin can be further divided into two fault blocks by a intrabasinal fault striking NE: northern block (abbreviated as N block) and southern block (abbreviated as S block) (Figs. 1 and 2). The sequence of strata in the N block is generally repeated also in the S block. However, variations in thickness and facies of constituent rocks are recognized between the blocks (Figs. 1 and 3). These features imply that the subsidence rates in each block were different, even if they could have been subsided contemporaneously.

Three chronostratigraphic key markers are observed in the NE subbasin (Figs. 1 and 4). They are one dacitic fallout tuff layer in the Kampo Conglomerate and two basaltic flows (the lower and the upper basaltic lavas) in the Eoil Formation. The fallout tuff layer in the Kampo Conglomerate has a relatively constant thickness of about 8 m. It can be traced laterally from the N block to the S block, even though its continuity is partly truncated by faults. And the thickness and facies of sedimentary rocks in the uppermost part of the Kampo Conglomerate are almost the same in both fault blocks. The facies is mostly pebbly sandstones with a constant thickness of about 10 m. These features suggest that the N and the S blocks were subsided probably as a single coherent fault block with the same subsidence rate during the deposition of the Kampo Conglomerate.

However, the thickness and facies of constituent members of the Eoil Formation become varied considerably throughout the Eoil Basin (Figs. 1 and 3). Particularly noticeable is the variation in thickness and facies of the tuffites deposited between the lower and upper basaltic lavas. Their characters depend on which the fault blocks they are located: In the S block, most of the rocks are tuffaceous conglomerates and have a maximum thickness of about 250 m (estimated from outcrop width and dip magnitude). The thickness is decreasing from the center toward northeastern and southwestern margins and two basaltic lavas are finally in contact in the northeastern part (Fig. 1). In the N block, the rocks consist mainly of tuffaceous sandstones with the maximum thickness of about 10 m, which is even thinner than that in the S block. These features indicate that the N block and the S block experienced different subsidence rates as two separated blocks after the first effusion of the basaltic lava.

Meanwhile, the upper basaltic lava of the Eoil Formation is partly exposed in the northeasternmost part of the SW subbasin. It shows pinch-out termination toward SW. This imply that the SW subbasin was not subsided during the deposition of the Eoil Formation with the exception of the northeasternmost area of the SW subbasin.

The basin-fills overlying the upper basaltic lava are tuffaceous sandstones and agglomerates. These two rocks are intertonguing in the central areas of the N and S blocks. They gradually change into the lacustrine sedimentary rocks upwards. The outcrop widths of the tuffaceous sandstones and agglomerates in the S block are slightly broader than those in the N block.

The Songjeon Formation is distributed both in the NE and in SW subbasins. In the NE subbasin, only some conglomerates are exposed in the highlands, while in the SW subbasin the brackish water sandstones are found additionally (Figs. 1 and 3). The conglomerates and sandstones in the SW subbasin have maximum thicknesses of about 120 m and 350 m, respectively. It is noticeable that breccias occur only along the southeastern border faults of the SW subbasin and they are intertonguing with the sandstones.

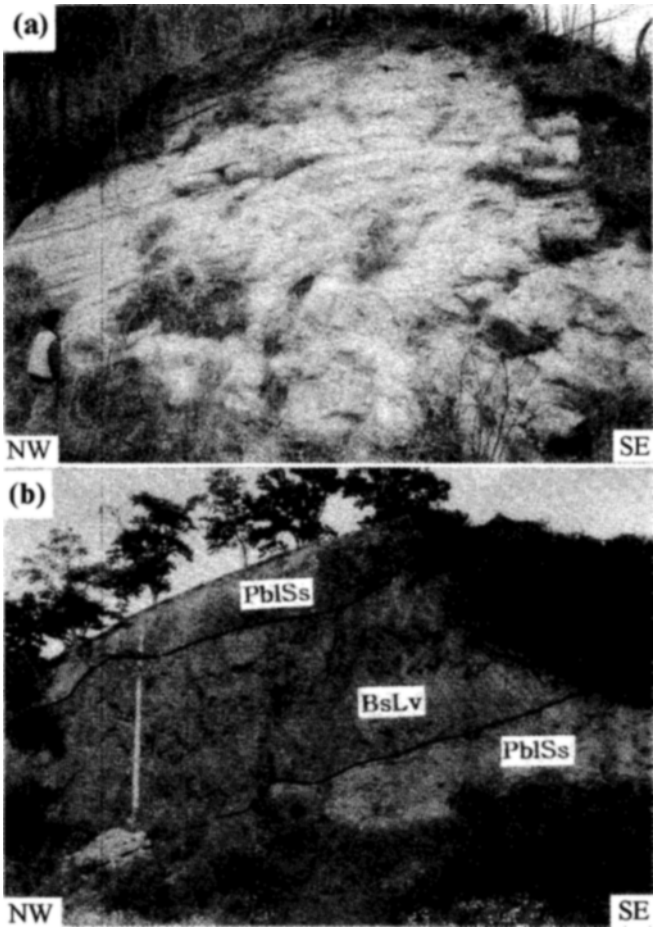

Fig. 4. Outcrop photographs of the chronostratigraphic key beds in the Eoil Basin. (**a**) Acidic fallout tuff in the upper part of the Kampo Conglomerate. It is crudely stratified, pumice-rich and gradually changes into pebbly sandstones upwards. (**b**) The lower basaltic lava in the Eoil Formation. It is concordant with sedimentary rocks above and below. In the sedimentary rocks above, cut-and-fill structures and basaltic rip-up clasts are observed. PblSs: pebbly sandstone, BsLv.: basaltic lava.

4. STRUCTURAL ARCHITECTURE

4.1. Stratal Geometry

The attitude of bedding generally defines a homoclinal structure dipping toward NW, although intrabasinal folding and faulting somewhat complicate this pattern (Figs. 2 and 5). The general dip of bedding is 15°–30° NW in the Eoil

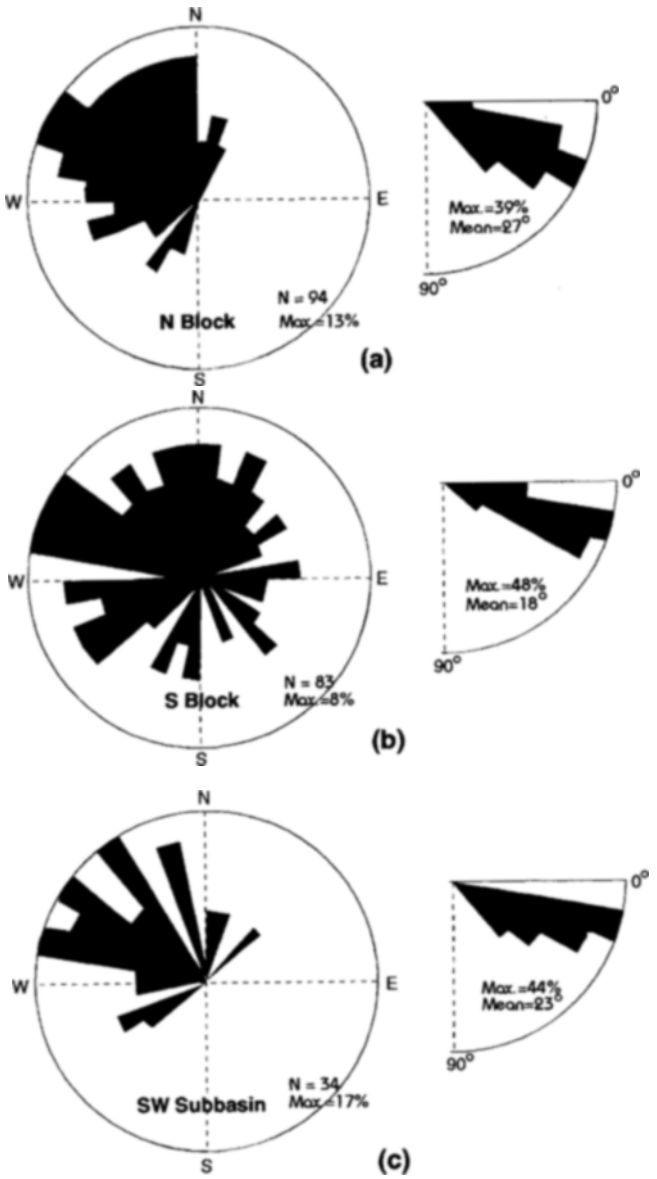

Fig. 5. Rose diagrams showing dip direction and dip value of bedding planes. See text for detailed explanation.

Basin. In the N block, the average dip angle is 27° mostly toward NW, slightly steepening toward northwestern border fault (Figs. 3 and 5a). This may imply a reverse drag fold (rollover anticline) caused by listric faulting of the northwestern border faults. In the S block, however, dip directions are more scattered with the average dip angle of 18° (Fig. 5b). It is probably due to major intrabasinal folds as well as simple drag folds adjacent to intrabasinal normal faults. In the northwestern central part of the S block, southeasterly dipping strata are recognized (Fig. 2). This may imply a simple drag fold generated by NE-trending intrabasinal normal faulting.

In the SW subbasin, the average dip is 23°, less than that in the N block but more than that in the S block. The dip directions are mostly NW (Fig. 5c).

4.2. Basin-bounding Faults and Intrabasinal Faults

As a whole, the Eoil Basin has an elongated shape. It is bounded with basement rocks by fault segments ranging from about 0.25 to 7 km in length (Figs. 1 and 2). The border fault systems are of two types: (1) normal faults trending NE–ENE and (2) dextral strike-slip faults trending NNW. The normal faults define the northwestern and southeastern margins of the Eoil Basin and are often expressed as fault-line scarps topographically. The dextral strike-slip faults define the northeastern and southwestern margins of the basin and subbasins.

The northwestern border faults of the NE subbasin are expressed by a fractured zone of about 20 m width and generally dip 60°–70° toward SE. They can be recognized by the fault line scarps and predominance of minor faults near them. These border faults consist of two main segments: the western part trending about N25°E and the eastern part trending about N80°E. The western part is generally straight. The eastern part, however, has partly a convex surface trace toward N, which seems to guide the traces of volcanic vents (Chwae et al., 1988). The slip-sense indicators on the fault surfaces indicate that dip-slip normal faulting was a main component (WT1, WT3, and WS2 in Fig. 10, as will do detailed explanations in the next section). Along the eastern part, sinistral strike-slips are recognized together with dip-slip (WS2 in Fig. 10).

The southeastern border faults of the NE subbasin are expressed as about 10 m wide fractured zone, and generally dip 60°–70° toward NW with mostly NE strike (Fig. 2). The border faults seem to have been active as antithetic faults (terminology of Gibbs, 1984) to the northwestern border faults. The developments of fault-line scarps are relatively meagre in contrast to the northwestern border faults. This may imply that the amount of vertical displacement of these faults was less than that of the northwestern border faults. The indicators of slip-sense show dip-slip normal faulting in general. Figure 6a shows a southeastern border fault which strikes N20°E and dips 68°NW. This fault, which is a contact between the Kampo Conglomerate and the basements, has a normal fault geometry and shows a thick fault gouge zone of about 6 m wide. Adjacent to the fault, it is shown that the pebbles of the Kampo Formation are angular and poorly sorted. Most of the pebbles consist of rhyolitic welded tuffs derived from nearby basement rocks.

The northwestern and southeastern border faults of the SW subbasin have similar features to those of the NE subbasin (WS3 and WS4 in Fig. 10). They make a feature of fault-line scarps generally and the widths of fracture zones are about 10–20 m. The northwestern border faults dip 60°–70° toward SE, while the southeastern ones, as antithetic

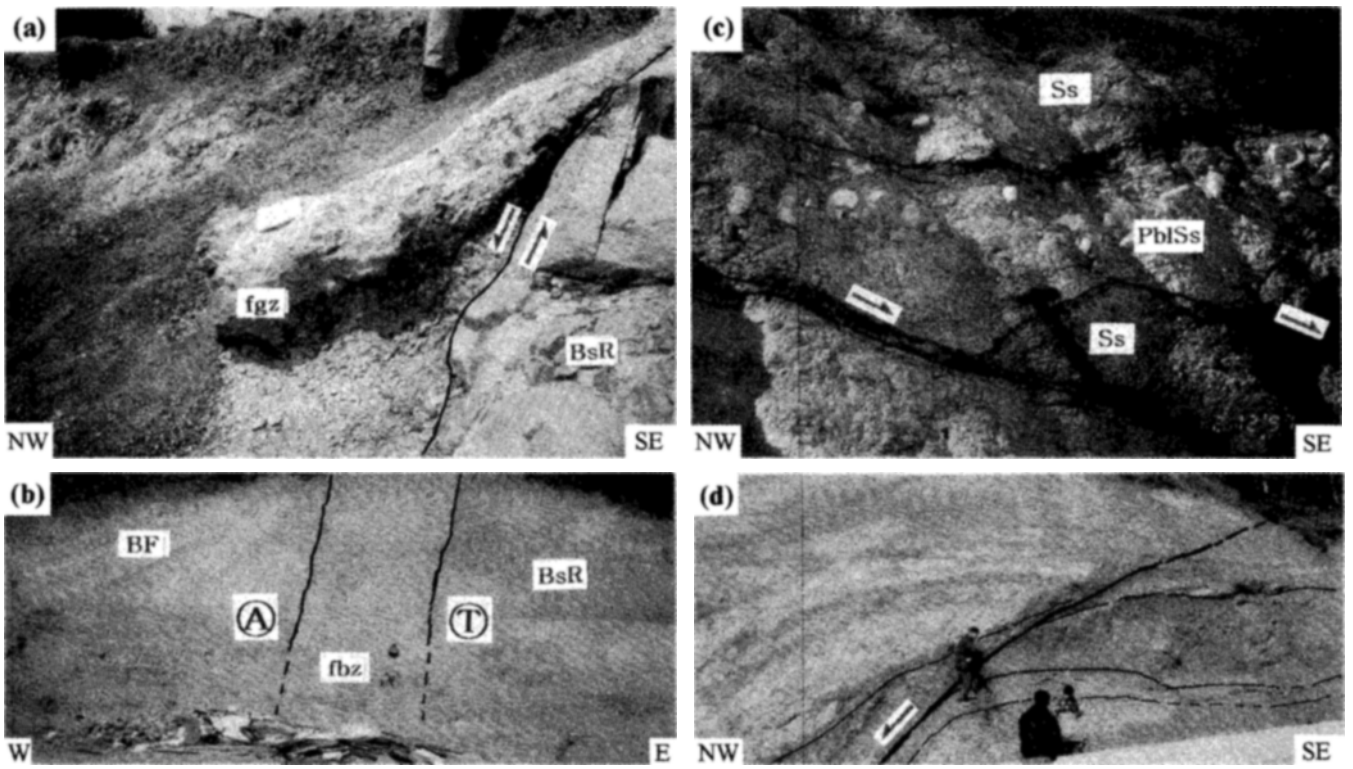

Fig. 6. Outcrop photographs of major faults and basin-fill sediments. (**a**) A southeastern border fault of the NE subbasin. (**b**) A northeastern border fault of the NE subbasin. (**c**) Minor growth faults in the basin-fills near the fault of **b**. This is one of a number of field evidences which suggest NW–SE extension of the Eoil Basin. (**d**) A major intrabasinal fault dipping toward northwest. Drag fold indicates dip-slip normal faulting. See text for further explanations. fgz: fault gouge zone, BsR: basement rocks, PblSs: pebbly sandstone, BF: basin-fills, fbz: fault brecciated zone, Ss: sandstone, Ⓐ: away from the reader, Ⓣ: toward the reader.

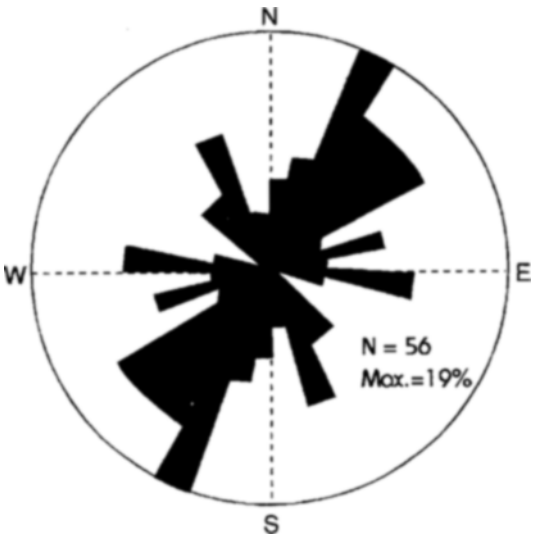

Fig. 7. Rose diagram showing strikes of all mappable faults in the study area. Majority of the faults is NE-trending normal faults, which suggests NW–SE extension of the Eoil Basin. The second mode in the diagram represents NNW-trending strike-slip faults.

faults to the northwestern border faults, dip toward NW. It is characteristic that there are some economic deposits of clay minerals, especially bentonites, along the both border faults, which indicate prevalent hydrothermal activities along the fault zones.

Meanwhile, the dextral strike-slip fault system trending NNW divides the Eoil Basin into two subbasins (the NE subbasin and the SW subbasin) and makes the northeastern and southwestern margins of the basin (Fig. 2). The northeastern border fault of the basin, which can be observed near #31 national road, has the crushed zone of above 15 m wide (Fig. 6b). The fault dips about 80° toward SW. Dextral strike-slips along the fault planes trending NNW are main component and NW–SE extension is recognized (KC1 and WS1 in Fig. 10). Minor growth faults trending NE are often observed within the basin-fills (the Kampo Conglomerate) near the fault (Fig. 6c and KC1', KC2 in Fig. 10). The basin-fills near the fault consist of conglomerates and pebbly sandstones. The clasts, which consist mainly of the fragments derived from nearby basement rocks, are mostly angular and matrix-supported. These are in contrast with the general features of the Kampo Conglomerate which clasts are subrounded-subangular and clast-supported. These facts should indicate that the fault was active contemporaneously with sedimentation. In the southwestern margin of the basin, crushed zone formed by faulting is about 20 m wide, and can be

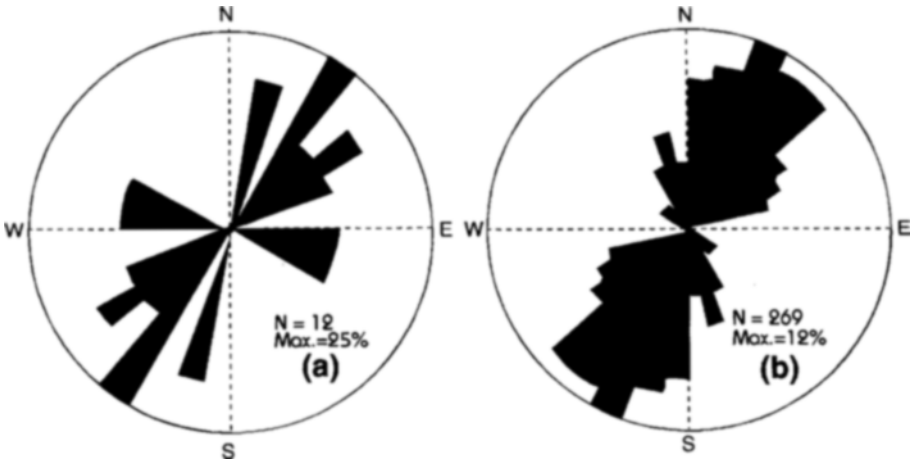

Fig. 8. Rose diagrams of (**a**) strikes of mafic dikes which have intruded the basement rocks surrounding the Eoil Basin, and (**b**) strikes of minor faults, being mostly normal faults, within the basin. Note that their main trends are NNE–NE, which suggest NW–SE extension of the Eoil Basin.

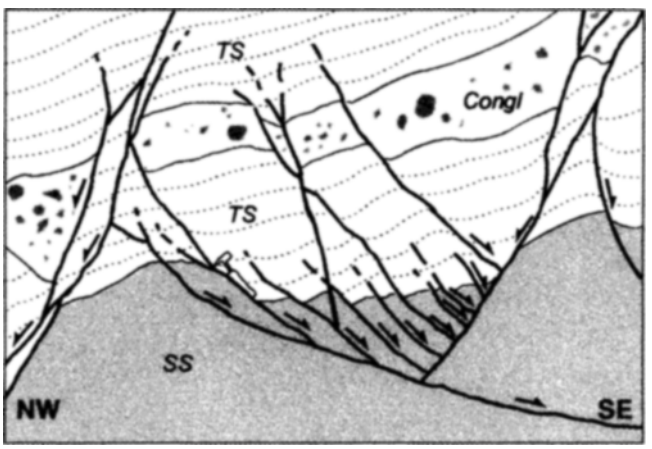

Fig. 9. Sketch of an outcrop showing a typical set of syndepositional normal faults with NE trend. Note the extensional structures such as listric faults, listric fan, antithetic faults, and half-grabens. See the hammer near the center of the picture for scale. Most of normal faults is concealed by the upper sediments, providing constraints on the timing of fault activity. Note that beds in the hangingwall is more thicker than those in the footwall (Note especially conglomerate bed). Congl: conglomerate, TS: tuffaceous sandstone, SS: sandstone.

traced continuously. Meanwhile, the fault dividing the Eoil Basin into two subbasins cannot be directly observed in the field because of thick alluvial cover. We can infer, however, the existence of the fault from the geological map showing sudden and unlikely changes in lithology over the suspected line (Fig. 1). Adjacent to the fault, about N30°E-oriented horizontal maximum stress is calculated by using the fracture analysis of Choi (1991) (HG1 and WT2 in Fig. 10).

In the central part of the NE subbasin, NE-trending intrabasinal faults are observed (Figs. 1 and 2). Most of them are synthetic faults to the northwestern border faults, even though some are antithetic. Figure 6d shows an antithetic normal fault accompanied by a simple drag fold. Most of antithetic intrabasinal faults are generally developed in the more northwestern side than the synthetic ones (Fig. 2). Thus, the synthetic and antithetic faults in the central part of the NE subbasin must have made a sort of central graben high (Fig. 3; terminology of Gibbs, 1984).

Trends of mappable fault segments including the border faults and the intrabasinal faults of the Eoil Basin are illustrated in a rose diagram (Fig. 7). In general, NE-striking faults, which are normal faults, are most dominant; a few have NNW or E–W trend.

4.3. Intrabasinal Folds

Even though the stratal attitudes in the Eoil Basin are partly disturbed by local faults, two types of folds are recognized in the NE subbasin (Fig. 2): (1) simple drag folds originated by the movement of adjacent major faults and (2) transverse folds with their axes generally perpendicular to the strikes of the northwestern and southeastern border faults. Such transverse faults have been reported in the Triassic–Jurassic rift basins, such as in the Newark basin of eastern North America (Schlische, 1992, 1993).

In the southwestern area of the NE subbasin, a series of simple drag folds are recognized along the NNW-trending border fault which separates two subbasins (Fig. 2). Their axes strike NNW or N–S being oblique 10°–30° to the border fault. Geometry of the folds is an asymmetrical synclinal shape with axis plunging toward N. These drag folds seem to have been originated by the dextral strike-slip motion of the border fault. In the central part of the NE subbasin, a NE-trending drag fold is observed along the intrabasinal faults. It has a symmetrical synclinal shape and its axis is parallel to the strikes of the adjacent faults. This probably implies that it has been originated by the normal faulting of the intrabasinal faults dipping toward SE.

Transverse folds, synclines and anticlines, are also developed in the NE subbasin (Fig. 2). Their axes are roughly perpendicular to the long dimension of the Eoil Basin and plunge about 5°–20° toward NW or WNW. The N block corresponds

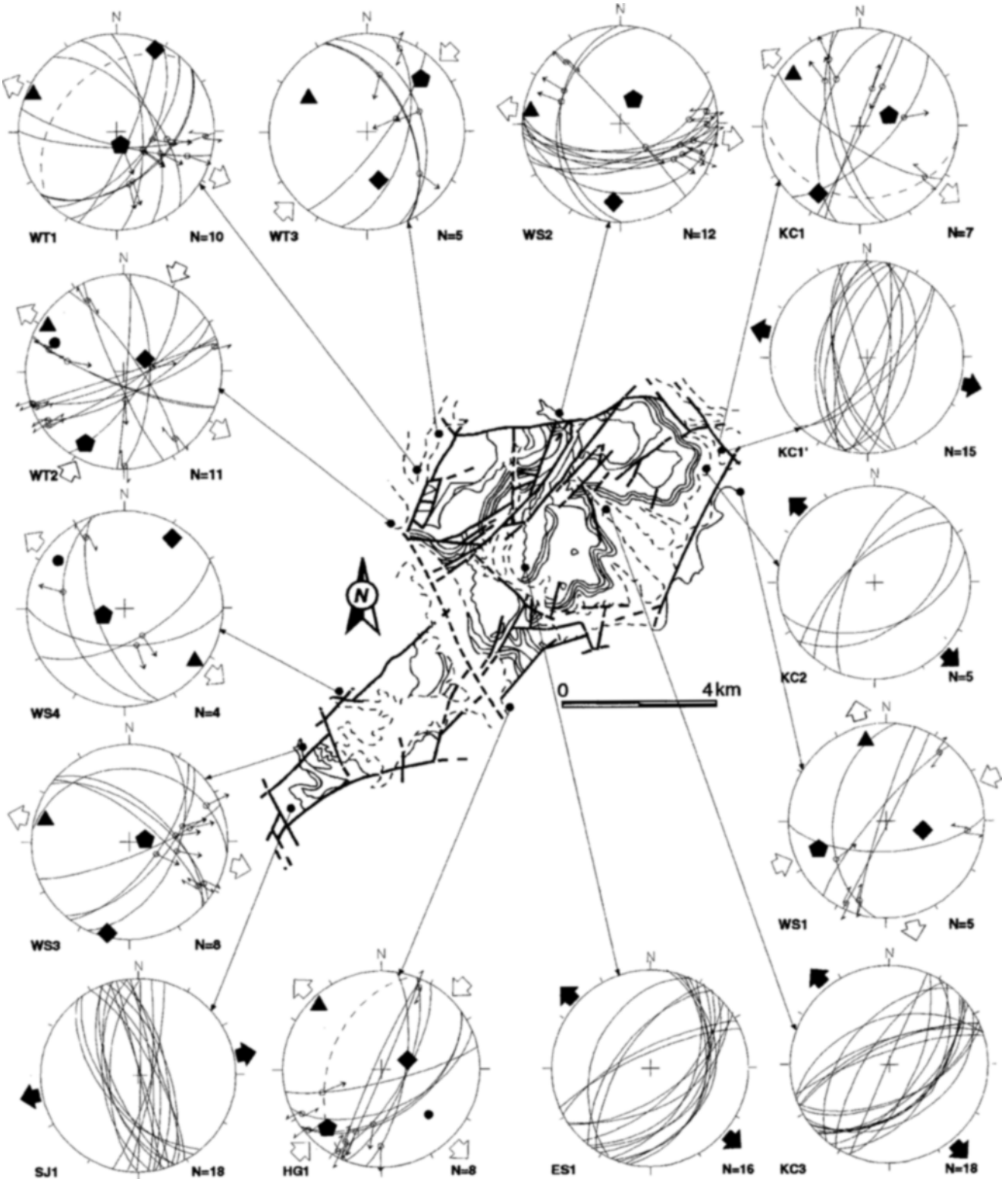

Fig. 10. Fault-slip and conjugate band data in the basements adjacent to the border faults and in the basin-fills (lower hemisphere, equal-area projections). Divergent arrow and convergent arrow heads represent horizontal stretching (σ_{Hmin}) and contraction directions (σ_{Hmax}), respectively. Open arrows are for directions calculated by using the fault tectonic analysis (DAGUR) of Choi (1991), filled arrows are for directions inferred from the geometry of the conjugate deformation band sets. When determined, the principal stress axes σ_1 (filled pentagons), σ_2 (filled squares), σ_3 (filled triangles) are also projected. Filled circles are poles to the intrusion planes of mafic dikes. Dotted great circles are the projections of bedding. HG: Cretaceous Hayang Group, WS: Wangsan Formation (Paleocene–Eocene acidic volcanics), WT: Waupri Tuffs, KC: Kangdong Conglomerates, ES: Tuffaceous sandstones in Eoil Formation, SJ: Songjeon Formation.

to the hangingwall of the northwestern border faults, and the S block to the hangingwall of the main intrabasinal faults as well as the southeastern border faults. All of these faults are normal faults. The faults themselves do not appear to be folded, and folds are not present in the basement. These features indicate that the folds appear to be generated during the basin subsidence, not by any later compression.

In the N block, transverse folds are generally plunge about 20° toward WNW (Fig. 2). Their amplitude is largest, as a synclinal shape, nearby the junction of two northwestern border fault segments and generally decreases away from the border faults. In the northeastern area of the S block, the axes of transverse folds plunge about 10° toward NW. The shallower plunges in the S block seem to be due to the different magnitude of tilting between the two blocks. Like the case in the N block, the amplitude of the folds are largest nearby the junction of two different-trending faults and slightly decrease away from the faults. These facts seem to mean that the geometry of transverse folds are intimately influenced by that of adjacent major faults.

As noted above, the trend of axial traces of transverse folds generally ranges from N45°W to N70°W (Fig. 2). It is oblique about 20°–50° to the NNW-trend of the strike-slip fault system. This orientation pattern is compatible with that of the secondary folds induced in the NNW dextral strike-slip tectonic regime (Wilcox et al., 1973; Allen and Allen, 1990; and others).

4.4. Mafic Dikes, Minor Faults, and Reconstruction of Paleostress Fields

Even though it was not possible to find any dike within the basin-fills themselves of the Eoil Basin, several mafic dikes have been observed in the adjacent basement rocks. They seem to have intruded into basement contemporaneously with the basaltic lava flows within the basin, considering similar lithology. Most of their intrusion planes trend toward NE (Fig. 8a). This direction is generally parallel to the strikes of the major mappable normal faults in the Eoil Basin. In addition, it is almost perpendicular to the average dip direction of the basin-fills and to the axes of transverse folds.

A large number of small-scale faults, which often make graben or half-graben geometries, are observed in the basin-fills. Most of them are NE-striking, and some NNW-striking faults are observed (Fig. 8b). The main strikes of the faults are the same as the predominant trend of the mafic dikes as well as those of the dominant mappable faults. They are often syndepositional normal faults (Fig. 6c). Figure 9 shows a typical set of syndepositional normal faults trending NE and having extensional structures of Gibbs (1984), where listric fault geometry, listric fan, antithetic fault, and outcrops-scale half-grabens are clearly observed. Most of normal faults do not penetrate the upper sediments, and the beds in the hangingwall are thicker than those in the footwall (Note the conglomerate bed in Fig. 9). The separation of beds tends to be decreased in the upper layer.

From fracture systems observed on total 14 outcrops of basements adjacent to the border faults and of the basin-fills, we determined the paleostress fields, the orientations of the principal stress axes ($\sigma_1>\sigma_2>\sigma_3$) and their horizontal projections (σ_{Hmax} and σ_{Hmin}) (Fig. 10). In favorable sites where enough striated fault planes are exposed, mostly in the basements adjacent to the border faults, determination of the orientations was done by using the fault tectonic analysis methods of Choi (1991). Slip sense was determined by using well-known indicators like orientations of fault-related minor fractures, mineral fibers, dragging of preexisting planar structures, piercing points, etc (Petit, 1987; Doblas et al., 1997; Doblas, 1998) (Fig. 11a–c). In other sites, mostly in the basin-fills which are almost unconsolidated, only approximate orientations were evaluated by using conjugate deformation band (band fault) sets which make (half) graben or horst geometries (Fig. 11d).

Since the major border faults are almost totally crushed zone and are not exposed as single fault planes, we used an indirect approach, determining the stress fields recorded in rocks exposed nearby the faults. Indeed, the stress fields can constrain movement along major faults (Hancock and Barka, 1981; Fabbri et al., 1996). Our analysis shows that the movements of all border faults occurred under a consistent stress field of a NE–SW-directed compression and a NW–SE-directed tension (Fig. 10). For all sites adjacent to the border faults (HG1, WS1, WS2, WS3, WS4, WT1, WT2, WT3, KC1), σ_1 or σ_2 is vertical or subvertical and σ_{Hmax} trends NE and σ_{Hmin}, NW. The stress field calculated by using all striated fault planes of all sites shows that σ_1 is subvertical and that σ_{Hmax} trends about N34°E and σ_{Hmin} about N56°W (Fig. 12). The stress ratio R ($\sigma_2-\sigma_3/\sigma_1-\sigma_3$) is 0.744, which means a transtensional stress field (Delvaux et al., 1997). These are compatible with that the northwestern and southeastern border faults were active as normal faults and the northeastern and southwestern border faults as dextral strike-slip faults.

Since the basin-fills are almost unconsolidated, it is difficult to observe enough striated fault planes. However, conjugate family of deformation bands, which show normal separations in sectional view, are often present in fine-grained sedimentary rocks (KC1', KC2, KC3, ES1, SJ1 in Fig. 10 and Fig. 11d). These can be utilized for determining the stress field during shear and volume reduction of highly porous sandstones (Aydin and Johnson, 1983; Mair et al., 2000). Our analysis shows that for four sites (KC1', KC2, KC3, ES1) NW–SE-directed extension is dominated, which is consistent with the results calculated by using striated fault planes as well as the main trends of mafic dikes and mappable normal faults. One exception, which was gathered in the youngest Songjeon Formation adjacent to the southwestern border fault (SJ1), shows ENE–WSW-directed extension. This trend is almost perpendicular to that of the border fault.

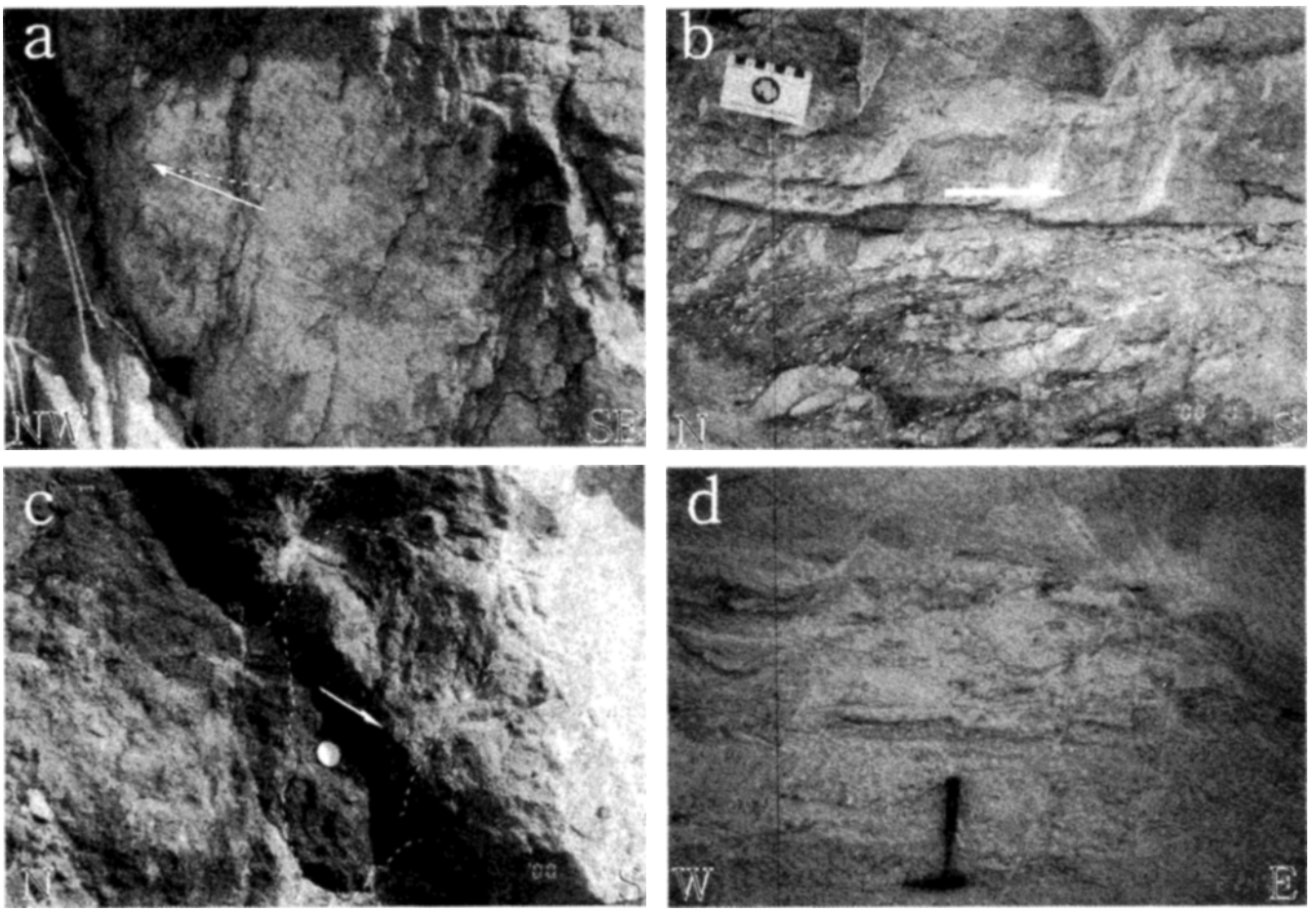

Fig. 11. Photographs showing slip-sense indicators and typical conjugate family of deformation bands. (**a**) Secondary R fractures indicating a dextral strike-slip movement in the Paleocene–Eocene acidic volcanics. White arrow indicates the movement direction of missing block. Dotted line represent a horizontal line. (**b**) Dragging of preexisting joints indicating a top-to-the-right movement in the Waupri Tuffs. (**c**) Separation of elongated clast, as a piercing point, indicating a sinistral strike-slip movement in the Waupri Tuffs. White arrow indicates the movement direction of left block. (**d**) a typical conjugate family of deformation bands (band faults) in the Songjeon Formation showing normal separations and graben (or horst) geometries in sectional view.

It remains questionable whether the trend means a local stress field affected by relative subsidence of eastern block along the fault or a more recent stress field recorded in the youngest formation. Indeed, as will be discussed in the next section, NW–SE-directed extension was no more active after the Songjeon Formation was deposited (after about 15 Ma).

In summary, all these facts suggest that most of minor faults (deformation bands), mafic dikes, and major mappable faults were formed coevally and under a uniform stress field, and that the transtensional stress field with a NE–SE-directed compression and a NW–SE-directed tension was prevalent during Early–Middle Miocene period in and around the Eoil Basin.

5. DISCUSSION

In this section, structural and stratigraphic observations will be combined to examine the followings: (1) timing of main structural developments (i.e., border faults, intrabasinal faults and folds) relative to sedimentation, (2) extension direction of the basin (3) evolution history of the basin.

5.1. Timing of the Structural development

The present body of evidences suggests that most of the main structures in the Eoil Basin were syndepositional, even if some could be at least sporadic. In the NE subbasin, the strata are tilted (about 20°), thickened, become younger toward the northwestern border faults, and showing generally a homoclinal structure (Figs. 1, 2 and 3). This pattern suggests such a wedge shaped half-graben structure, which have been reported in a number of the fault-bounded basins worldwide, for example in the basins of the Basin and Range Province of North America (Wernicke and Burchfiel, 1982; Allen and Allen, 1992) as well as in other Korean Miocene basins such as in the Chongja basin (Son and Kim, 1994). If the northwestern border faults are syndepositional,

then a progressive decrease in dip angle toward the younger strata is expected (Fail, 1988). Even though systematic decrease in dip angle across the basin is difficult to be observed due to the effect of the intrabasinal faulting and folding, Chwae et al. (1988) reported that the youngest Songjeon Formation dips about 5°–10° with the lowest angle among the basin-fills and overlies the lower strata angular-unconformably. In the NE subbasin, our observations are consistent with their results. The attitude of the Songjeon Formation are almost horizontal there. These facts indicate that there were more than one tilting events in the NE subbasin between depositions of the Songjeon and Eoil Formations, and that the northwestern border faults of the NE subbasin are, therefore, syndepositional at least sporadically.

As mentioned above, the NE subbasin is divided into the N block and the S block by intrabasinal normal faults. Before effusion of the first basaltic lava, thickness and facies of sedimentary rocks (in the Kampo Conglomerate) were generally the same in both blocks (Figs. 1 and 3). After the first basalt effusion, however, the thickness and facies of sedimentary rocks (in the Eoil Formation) in both blocks become quite different. Especially the tuffites in the S block deposited between the lower and upper basaltic lavas were much thicker than those in the N block. It is inferred from this fact that the block-bounding intrabasinal faults are syndepositional, and that the faults, therefore, must have begun to act as large growth faults since the first effusion of basaltic lava.

Meanwhile, along the southeastern and northeastern border faults of the NE subbasin, abnormal clasts of high angularity are observed. This is in contrast with the general roundness of the fluviatile Kampo Conglomerate in the basin. In addition, small-scale growth faults and deformation bands (KC1 and KC1' in Fig. 10) are observed in the basin-fills adjacent to the border faults. These features seem to be related with the syndepositional faulting of the faults.

All of observed extensional features including mappable normal faults, mafic dikes, small-scale growth faults, and conjugate family of deformation bands consistently indicate a NW–SE directed extension. Besides, all stress fields calculated by using striated fault planes adjacent to the border faults are also compatible with the result. These facts reflect that all of them were formed coevally under a uniform stress field.

As for the SW subbasin, breccias are distributed only adjacent to the southeastern border faults. They are very angular and poorly sorted. The maximum diameter of the clasts amounts to a few meter near the border faults, and decreases dramatically toward NW. On the contrary, the northwestern border faults are contacting directly with well-sorted sandstone layers (the Songjeon Formation) which consist mainly of fine sand grains and contains abundant molluscan fossils. The general dip angles of the strata (about 23°NW) in this SW subbasin are obviously higher than those in the NE subbasin where they are almost horizontal. This means that the SW subbasin experienced a later northwestward tilting event after the deposition of the Songjeon Formation. These suggest that the southeastern border faults are syndepositional, while the northwestern border faults might be postdepositional. Meanwhile, comparing the ages of basin-fills in the two subbasin and considering the pinch-out termination of the basaltic lavas in the northeastern part of the SW subbasin, it can be concluded that the activities of the major faults in the NE subbasin preceded those in the SW subbasin.

Based on the listric fault models (Wernicke and Burchfiel, 1982; White et al., 1986; Grosong, 1989; Dula, 1991) as well as on the assumption of two listric fault surfaces of constant curvature, building a basin margin and intersecting obliquely, Scott et al. (1994) calculated their 'track' which was defined by the intersection line of the two fault surfaces, and calculated the dip pattern of the hangingwall surface. They concluded that (1) a syndepositional ridge (anticline) is created on the hangingwall surface over the 'track', and (2) the 'track', which is traced by the axis of the anticline, is clearly linear and establishes the kinematic path of the block as well as the direction of maximum horizontal extension. Meanwhile, Schilsche (1992, 1993) argued in the Triassic–Jurassic continental rift basins of eastern North America that the syndepositional folds (syncline and anticline) can be formed due to the differential displacement of border fault-segment just like the tip line loop theory (Barnett et al., 1987). He substantially observed in the field that syndepositional anticlines were developed in the intersection points of border fault-segments. Our observed folds in the Eoil Basin, especially transverse folds, should be synsedimentary just like the results of the above mentioned studies. It is substantiated by the facts that only the basin-fills are folded, while the adjacent faults and the basement are not folded. In addition, amplitudes of the folds generally decrease away from the border faults, implying that the genesis of folds are intimately related with the movement of adjacent border faults. On the other hand, our observations show that in the intersection point (corner) of two different-trending border faults large-scale synclines rather than anticlines are formed (Fig. 2). It indicates more subsidence at the corner and decreasing subsidence away from there. It is not concordant with the results of the previous studies (Scott et al., 1994; Schilsche, 1992, 1993). A reason of this discrepancy can be ascribed to the internal deformation of the basin due to a sinistral oblique-slip along the eastern segment (trending as about N80°E) of the northwestern border fault of the NE subbasin, whose evidence is observed in the field (WS2 in Fig. 10). If oblique-slip is true, it is inferred that the trend of the eastern segment of the northwestern border faults is not aligned perpendicularly to the extensional direction of the basin. The strike-slip component hindered the vertical displacements of the hangingwall blocks in the northeastern margin of the basin. On the other hand, more subsidence at the corner can also be ascrib-

ed to the volcanic vents of the basaltic lavas located near the corner (Chwae et al., 1988). The vents might have caused a kind of nested cauldron structure spouting much materials from the underneath (Kim, C.S. and Yamauchi. S., 1997: personal communications).

In summary, most of the main structures (faults and folds) in the Eoil Basin were active, at least sporadically, in parallel with sedimentation. One exception might be the northwestern border faults of the SW subbasin. Syndepositional structures, each of which was active at different time, must have strongly controlled the location of depocenter, basin capacity, sediment supply rate and sedimentary environments.

5.2. Extension Direction of the Basin

Stratal geometry in the rift basins as well as in the pull-apart basins generally depends on the geometry of border faults, and reflects the tilting aspect of basement and the extension direction of the basins (Wernicke, 1981; Wise, 1992; Schlische, 1993; Lucchitta and Suneson, 1993). It has been well-known that the average dip direction of basin-fills is opposite to tectonic transport direction, although internal deformations could slightly alter this pattern (Scott et al., 1994). The average dip direction of the strata in the Eoil Basin is N40°W. This means that the hangingwall blocks of the main normal faults have been transported toward SE.

Several mafic dikes were observed in the basement rocks of neighboring area. Most of their intrusion planes are arranged toward N30°–60°E (Fig. 8a). This trend is nearly the same as that of mafic dikes distributed near the Miocene Chongja Basin to the south of the Eoil Basin, which was interpreted as a result of NW–SE extension due to the regional NNW dextral shearing (Son and Kim, 1994). The trend is also similar to that of the ENE dike swarm in the Changgi Peninsula to the north of the Eoil Basin, which was considered as a result of NNW–SSE maximum tensional stress during the Early and Middle Miocene (Kim et al., 1991). The elongated shape of the Eoil Basin with NE axes (Figs. 1 and 2) is also suggestive to NW–SE extension. The basin consists of a series of parallelogram-shaped troughs (subbasins) bounded by normal faults striking NE or ENE. Within sedimentary strata, a number of small-scale normal faults are observed (Fig. 9), and many of them are growth faults which make small graben or half-graben geometries. Their main trend runs N30°–40°E (Fig. 8b). The paleostress field calculated by using striated fault planes shows that $_1$ is subvertical and that σ_{Hmax} trends about N34°E and σ_{Hmin} about N56°W (Fig. 12). The stress ratio R ($\sigma_2-\sigma_3/\sigma_1-\sigma_3$) is 0.744, which means a NW–SE transtensional stress field. Approximate stress fields evaluated by using conjugate deformation band (band fault) sets in the basin-fills show a NW–SE-directed extension. All of these features can be used to determine the direction of the maximum horizontal extension. It is, thus, concluded that the extension direction in the Eoil Basin area was NW–SE.

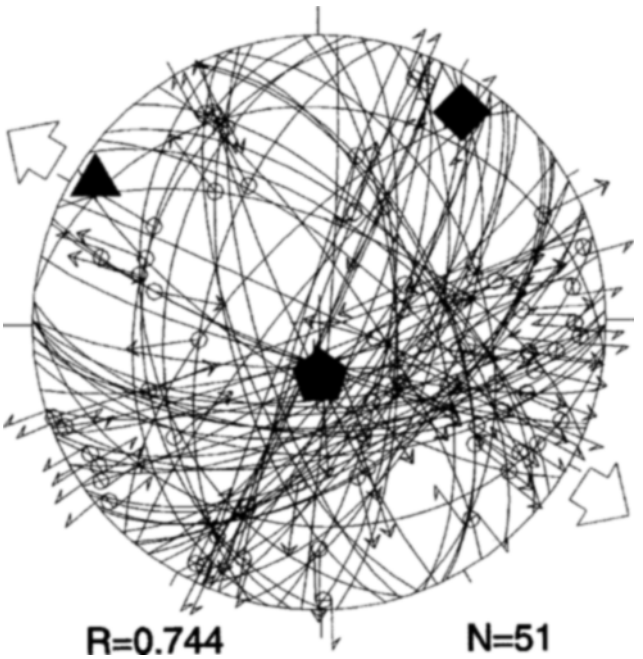

Fig. 12. Fault-slip data of all striated fault planes observed in the outcrops adjacent to the border faults (lower hemisphere, equal-area projections). Divergent arrow head represents horizontal stretching direction (σ_{Hmin}=N56°W). The principal stress axes σ_1 (filled pentagons), σ_2 (filled squares), σ_3 (filled triangles) are also projected. R: $(\sigma_2-\sigma_3)/(\sigma_1-\sigma_3)$.

During this extension, three NNW-trending faults (Fig. 2) played role of dextral strike-slip faults. Their trend is N20°–30°W, oblique about 50°–80° to the main trends of the normal border faults, small-scale growth faults, and mafic dikes and oblique about 50° to the trend of σ_{Hmax} (Fig. 12). If the NNW faults were active as the transfer faults in the rift basin of orthogonal extension origin, their strikes would be perpendicular to the extensional structures. If the NNW faults were the master faults in the pull-apart basin of strike-slip fault origin, one could expect that their strikes are oblique about 40°–50° to the extensional structures (Lister et al., 1986; Scott et al., 1994). Although the observations mentioned above are somewhat controversial to determine the exact character of the NNW faults, the orientation pattern is more resemblant to that in the pull-apart basin than that in the rift basin. In addition, the axes of the transverse fold (NW or WNW) are oblique about 20°–50° to the NNW faults. It is analogous to the orientation of secondary folds induced from a NNW–SSE dextral strike-slip tectonic regime (Wilcox et al., 1973; Allen and Allen, 1990; and others; Fig. 2). It is well-known from the previous paleomagnetic studies that there were pervasive clockwise rotations of remanent magnetic declinations in and around the Miocene basins during the Early Miocene–early Middle Miocene (Kim et al., 1986; Kim and Kang, 1989; Han, 1989; Son et al., 1996; and others). It means that

the tectonic regime at that time in the southeastern Korean Peninsula was dextral strike-slip fault regime. Thus, it is reasonable that the NNW faults of the Eoil Basin acted as master strike-slip faults rather than as transfer faults during the basin development, and that NW–SE extension was induced secondarily by a NNW–SSE dextral shearing.

5.3. History of the Basin Evolution

On the basis of the K–Ar whole-rock dating of basaltic lavas (18–20 Ma: Lee et al., 1992), the basin extension began in early Burdigalian time. This time is almost coeval with the extensions of the Ulleung and Yamato basins in the East Sea (Kaneoka et al., 1990; Chough and Lee, 1992; Jolivet and Tamaki, 1992). At the onset of the Eoil Basin extension, the normal faulting of the northwestern border faults of the NE subbasin were initiated, which was induced by the dextral strike-slip motions of the northeastern and southwestern border faults, perhaps together with the southeastern border faults. And then the block on the southeastern side of the faults slipped toward SE as a hangingwall wedge, creating an elongated trough trending NE, in which fluviatile deposits were accumulated. The total slip distance was increased quickly, and the trough grew in width and in depth through time. A concurrent result is the fining upward character of the Kampo Conglomerate. About at 20 Ma, the Eoil Basin may have experienced a quite rapid extension, resulting in the intrusion and effusion of basaltic lavas with accompanied slight uplift and creation of the intrabasinal faults in the NE subbasin. The intrabasinal faults divided the NE subbasin into the two main blocks (N block and S block). The blocks migrated continuously toward SE. Volcanic activities continued during sedimentation. These all activities created northwestward tilting of strata, syndepositional folding, variations of thickness and facies in the Eoil Formation, as well as the repetition of sedimentary sequences in the NE subbasin. Around the end of the Early Miocene, extension rate and volcanism became weaker and consequently the basin experienced thermal subsidence (McKenzie, 1978). The basin was filled by lacustrine sediments together with tuffs. And then, both the extension and volcanism stopped for some time.

Based on the early Middle Miocene age of the Songjeon Formation dated by *Vicarya-Anadara* molluscan fossils (Yoon, 1976), together with the angular unconformity relationship between the Songjeon and the Eoil Formations, it can be inferred that the extension must have resumed at the early Middle Miocene. The hangingwalls of the NE subbasin started to slip toward SE again. New fluviatile conglomerate sequence (lower part of the Songjeon Formation) was accumulated in the broadened space unconformably. On the other hand, it is inferable that the southeastern border faults of the SW subbasin were generated at that time, and this subbasin started to be extended and deepened rapidly. This resulted in inflow of sea-water through lowlands of the NE subbasin into the SW subbasin, as well as the lateral facies transition from breccias in front of the southeastern border faults to the sandstones northwestward. The latter is indicative of a nearshore brackish-water environment (Yun et al., 1989). Approaching to the final stage of the basin evolution, the northwestern border faults of the SW subbasin might have created, causing tilting of sequence of the strata toward NW.

We have, however, no field evidence for the termination time of the extension of the basin. Notwithstanding, the previous studies (Kim and Kang, 1989; Kim 1992; Son and Kim, 1994, 1996) allow us to conjecture that time. Those studies pointed out that the youngest rocks showing the clockwise deflections of the remanent magnetic declination have age of about 16 Ma. Son and Kim (1994) reported in the Miocene Chongja Basin that the growth faults of the basin do not cut through the uppermost portion of the early Middle Miocene sandstone sequence (the Shinhyon Formation). Additional paleomagnetic, heat flow, and radiometric age data from the Japanese Islands and the East Sea suggest that the East Sea stopped opening at 15 Ma (Otofuji et al., 1985; Tamaki, 1986; Tatsumi et al., 1990; Kim, 1992). Consequently, it can be concluded that the extension in the Eoil Basin stopped at about 15 Ma. Since than, the Eoil Basin has been uplifted by a tectonic inversion (Kim and Kang, 1996; Son and Kim, 1996; Son et al., 1996) and is continuously eroded until now.

6. SUMMARY AND CONCLUSIONS

(1) The Eoil Basin has an elongated shape and consists of a series of pull-apart type half grabens with NE axes. The basin is bounded on the northwestern and southeastern margins by a series of normal faults trending NE or ENE, and on the northeastern and southwestern margins by a series of dextral strike-slip faults trending NNW. The strike-slip faults acted as master faults of a pull-apart basin. The extension direction of the Eoil Basin is NW–SE. Based on our field observations and the results of previous studies, it seems that both the normal and strike-slip faults were generated by the NW–SE tensional stress induced secondarily by a NNW–SSE dextral shear stress acted in the study area from early Burdigalian to 15 Ma.

(2) The Eoil Basin is divided into two subbasin by a NNW-trending dextral strike-slip fault, i.e., the northeastern Eoil subbasin (NE subbasin) and the southwestern Eoil subbasin (SW subbasin). Based on lithofacies and ages of the basin-fills, it is concluded that two subbasins had different history of evolution. The NE subbasin is divided further into two fault blocks by a system of NE-trending intrabasinal normal faults. Each block experienced different subsidence history, even though almost contemporaneous.

(3) Most of our observations indicate that the main structures (border faults, and intrabasinal faults and folds) in the Eoil Basin were generally syndepositional, even if some of

them might have experienced at least sporadic motion.

(4) In the NE subbasin, two types of folds are recognized: simple drag folds with various orientation generated by the movement of the adjacent major faults and transverse folds with axes roughly perpendicular to the long axis of the basin. Among the transverse folds, the large-scale synclines are developed in the intersection point (corner) of two different-trending major faults. They may be related either with the internal deformation due to the sinistral oblique-slip along the eastern segment (striking about N80°E) of the northwestern border faults, or with a kind of nested cauldron structure.

(5) The general sequence of the main structure formation was as follows: firstly, the northwestern border faults of the NE subbasin (and possibly with the southeastern border faults of the NE subbasin); secondly, the intrabasinal normal faults of the NE subbasin and the intrabasinal folds; thirdly, the southeastern border faults of the SW subbasin; finally, the northwestern border faults of the SW subbasin.

ACKNOWLEDGEMENT: The authors wish to acknowledge the financial supports of the Korea Research Foundation made in program year of 1998 through the Research Institute for Basic Science, Pusan National University, Project No. 1998-15-D00264. And this research was partly carried out by the first author's Post Doctoral Fellowship (1998) of the Korea Research Foundation. We also express our thanks to the editors Prof. J.-H. Ree and Prof. D.K. Choi, and two reviewers, Dr. P.Y. Choi and Prof. J.H. Kang for their helpful comments on the manuscript.

REFERENCES

Adyin, A. and Johnson, A.M., 1983, Analysis of faulting in porous sandstone. Pure and Applied Geophysics, 116, 913–930.

Allen, P.A. and Allen, J.R., 1990, Basin Analysis: Principles and applications. Blackwell Scientific Publications, Oxford London, p. 115–140.

Barnett, J.A.M., Mortimer, J., Rippon, J.H., Walsh, J.L. and Watterson, J., 1987, Displacement geometry in the volume containing a single normal fault. American Association of Petroleum Geologists Bulletin, 71, 925–938.

Choi, P.-Y., 1991, Method for determining the stress tensor using fault slip data. Journal of Geological Society of Korea, 27, 383–393. (in Korean with English abstract)

Chough, S.K. and Lee, K.E., 1992, Multi-stage volcanism in the Ulleung back-arc basin, East Sea (Sea of Japan). The Island Arc, 1, 32–39.

Chwae, U.C., Hwang, J.H., Yun, U. and Kim, D.H., 1988, Geological report of the Eoil sheet, 1:25,000. Korean Institute of Energy and Resources, 41 p. (in Korean with English abstract)

Delvaux, D., Moeys, R., Stapel, G., Petit, C., Levi, K., Miroshnichenko, A., Ruzhich, V. and San'kov, V., 1997, Paleostress reconstruction and geodynamics of the Baikal region, Central Asia, Part 2. Cenozoic rifting. Tectonophysics, 282, 1–38.

Doblas, M., 1998, Slickenside kinematic indicators. Tectonophysics, 295, 187–197.

Doblas, M., Mahecha, V., Hoyos, M. and Lopez-Ruiz, J., 1997, Slickenside and fault surface kinematic indicators on active normal faults of the Alpine Betic cordilleras, Granada, southern Spain. Journal of Structural Geology, 19, 159–170.

Dula, W.F.Jr., 1991, Geometric models of listric normal faults and rollover anticline. American Association of Petroleum Geologists Bulletin, 75, 1609–1625.

Fabbri, O., Charvet, J. and Fournier, M., 1996, Alternate senses of displacement along the Tsushima fault system during the Neogene based on fracture analyses near the western margin of the Japan Sea. Tectonophysics, 257, 275–295.

Fail, R.T., 1988, Mesozoic tectonics of the Newark basin, as a view from Delaware River, In: Husch, J.M. and Hozik, M.J. (eds.), Geology of the Central Newark Basin. Field Guide and Proceedings: 5th Meeting of Geological Association of New Jersey, Rider College, Lawrenceville, New Jersey, p. 19–41.

Gibbs, A.D., 1984, Structural evolution of extensional basin margins. Journal of Geological Society of London, 141, 609–620.

Grosong, R.H.Jr., 1989, Half-graben structures: balanced models of extensional fault-bend folds. Geological Society of American Bulletin, 101, 96–105.

Han, J.H., Kwak, Y.H., Son, J.D. and Son, B.K., 1987, Tectonic evolution and depositional environment of the Tertiary sedimentary basin, southeastern part of Korea (II). Korea Institute of Energy and Resources, KR-86-2-(B), 109 p. (in Korean)

Han, J., 1989, Miocene Paleomagnetic Data from Southern Korea: Implication on Model for Opening of the Japan Sea. M.S. thesis, Texas A & M University, 132 p.

Hancock, P.L. and Barka, A.A., 1981, Opposed shear senses inferred from neotectonic mesofracture systems in the North Anatolian fault zone. Journal of Structural Geology, 3, 383–392.

Jin, M.S., Kim, S.J. and Shin, S.C., 1988, K/Ar and fission-track datings for volcanic rocks in the Pohang–Kampo area. Korea Institute of Energy and Resources, Research Report (KD-87-27), 51-88. (in Korean)

Jin, M.S., Kim, S.J., Shin, S.C. and Lee, J.Y., 1989, K/Ar and fission-track datings for granites and volcanic rocks in the southeastern part of Korean peninsula. Korea Institute of Energy and Resources, Research Report (KD-88-6D), 53–84. (in Korean)

Jolivet, L. and Tamaki, K., 1992, Neogene kinematics in the Japan Sea region and volcanic activity of the northeast Japan Arc. In: Tamaki, K., Suyehiro, K., Allan. J., McWilliams, M., et al. (eds.), Proceedings of the Ocean Drilling Program, Scientific Results, 127/128, Part 2, 1311–1331.

Kaneoka, I., Notsu, K., Takigami, Y., Fujioka, K. and Sakai, H., 1990, Constraints on the evolution of the Japan Sea based on ^{40}Ar–^{39}Ar ages and Sr isotopic ratios for volcanic rocks of the Yamato Seamount Chain in the Japan Sea. Earth and Planetary Science Letters, 97, 195–204.

Kang, H.-C., Kim, I.-S., Son, M. and Jung, H.-J., 1996, Palaeomagnetic study of sedimentary and igneous rocks in the Yangsan strike-slip fault area, SE Korea. Economic and Environmental Geology, 29, 753–765. (in Korean with English abstract)

Kim, B.K., 1970, A study on the Neogene Tertiary deposits in Korea. Journal of Geological Society of Korea, 6, 77–96. (in Korean with English abstract)

Kim, G.-S., Kim, J.-Y., Jung, K.-K., Hwang, J.-Y. and Lee, J.-D., 1995, Rb–Sr whole rock geochronology of the granitic rocks in the Kyeongju–Gampo area, Kyeongsangbugdo, Korea. Journal of Korean Earth Science Society, 16, 272–280. (in Korean with English abstract)

Kim, I.-S. and Kang, H.-C., 1989, Palaeomagnetism of Tertiary rocks in the Oil (Eoil) basin and its vicinities, southeast Korea. Journal of Geological Society of Korea, 25, 273–293. (in Korean with English abstract)

Kim, I.-S., 1992, Origin and tectonic evolution of the East Sea (Sea of Japan) and the Yangsan fault system: a new synthetic interpretation. Journal of Geological Society of Korea, 28, 84–109. (in Korean with English abstract)

Kim, I.-S., Son, M., Jung, H.-J., Lee, J.-D., Kim, J.-J. and Paik, I.-S., 1998, Geological characteristics of Kyongju–Ulsan: palaeomagnetism and magnetic susceptibility of the granitic rocks in the Ulsan Fault area. Economic and Environmental Geology, 31, 31–43. (in Korean with English abstract)

Kim, J.-Y., Jung, C.-Y. and Yoon, S., 1991, Early and Middle Miocene dike swarms and regional tectonic stress field in the Janggi peninsula. Journal of Geological Society of Korea, 27, 330–337. (in Korean with English abstract)

Kim, K.H., Won, J.K., Matsuda, J., Nagao, K. and Lee, M.W., 1986, Paleomagnetism and K–Ar age of volcanic rocks from Guryongpo area, Korea. Journal of the Korean Institute of Mining Geology, 19, 231–237.

Lee, H.-K., Moon, H.-S., Min, K.-D., Kim, I.-S., Yun, H. and Itaya, T., 1992, Paleomagnetism, stratigraphy and geologic structures of the Pohang and Changgi basins: K–Ar ages for the volcanic rocks. Journal of the Korean Institute of Mining Geology, 25, 337–349. (in Korean with English abstract)

Lee, Y.G., 1976, Fossil diatoms in the upper part of the Eoil Formation, Eoil area, Gyeongsangbuk-do, Korea. Journal of the Korean Institute of Mining Geology, 9, 77–84.

Lister, G.S., Etheridge, M.A. and Symonds, P.A., 1986, Detachment faulting and the evolution of passive continental margins. Geology, 14, 245–250.

Lucchitta, I. and Suneson, N.H., 1993, Dips and extension. Geological Society of America Bulletin, 105, 1346–1356.

Mair, K., Main, I. and Elphick, S., 2000, Sequential growth of deformation bands in the laboratory. Journal of Structural Geology, 22, 25–42.

McKenzie, D., 1978, Some remarks of the development of sedimentary basins. Earth and Planetary Science Letters, 40, 25–32.

Min, K.D., Kim, W.K., Lee, D.H., Lee, Y.S., Kim, I.-S. and Lee, Y.H., 1994, Paleomagnetic study on the Tertiary rocks in Pohang area. Economic and Environmental Geology, 27, 49–63. (in Korean with English abstract)

Otofuji, Y., Matsuda, T. and Nohda, S., 1985, Opening mode of the Japan Sea inferred from the paleomagnetism of the Japan Arc. Nature, 317, 603–604.

Paik, K.H., Woo, K.S. and Park, Y.A., 1992, Paleoceanography and paleoenvironment of the Middle Miocene Songjeon Formation, Yangnam basin, Korea. Journal of Geological Society of Korea, 28, 142–151.

Petit, J.P., 1987, Criteria for the sense of movement on fault surfaces in brittle rocks. Journal of Structural Geology, 9, 597–608.

Schlische, R.W., 1992, Structural and stratigraphic development of the Newark extensional basin, eastern North America: evidence for the growth of the basin and its bounding structures. Geological Society of America Bulletin, 104, 1246–1263.

Schlische, R.W., 1993, Anatomy and evolution of the Triassic–Jurassic continental rift system, eastern North America. Tectonics, 12, 1026–1042.

Schmid, R., 1981, Descriptive nomenclature and classification of pyroclastic deposits and fragments: recommendations of the IUGS subcommission on the systematics of igneous rocks. Geology, 9, 41–43.

Scott, D.L., Braun, J. and Etheridge, M.A., 1994, Dip analysis as a tool for estimating regional kinematics in extensional terranes. Journal of Structural Geology, 16, 393–401.

Son, M. and Kim, I.-S., 1994, Geological structures and evolution of the Tertiary Chongja basin, southeastern margin of the Korean Peninsula. Economic and Environmental Geology, 27, 65–80. (in Korean with English abstract)

Son, M. and Kim, I.-S., 1996, Palaeomagnetism of Tertiary basins in southern Korea: 2. basaltic rocks in the central part of Pohang basin. Economic and Environmental Geology, 29, 369–380. (in Korean with English abstract)

Son, M., 1998, Formation and Evolution of the Tertiary Miocene Basins in Southeastern Korea: Structural and Paleomagnetic Approaches. Ph.D. thesis, Pusan National University, 233 p. (in Korean with English abstract)

Son, M., Kang, H.-C. and Kim, I.-S, 1996, Palaeomagnetism of Tertiary basins in southern Korea: 3. Chongja–Ulsan basins and its vicinities. Economic and Environmental Geology, 29, 509–522. (in Korean with English abstract)

Son, M., Seo, H.-J., Jung, H.-J. and Kim, I.-S., 1997, Extension direction and tectonic boundaries of the Miocene basins, Southeast Korea. Tectonic Evolution of Eastern Asian Continent: Short papers for the International Symposium on the Occasion of the 50th Anniversary of the Geological Society of Korea, 104–109.

Tamaki, K., 1986, Age estimation of the Japan Sea on the basis of stratigraphy, basement depth, and heat flow data. Journal of Geomagnetism and Geoelectricity, 35, 427–446.

Tateiwa, I., 1924, 1:50,000 Geological Atlas of Chosen, No. 2, Ennichi, Kuryuho and Choyo sheets. Geological Survey of Joseon. (in Japanese)

Tatsumi, Y., Shigenori, M. and Nohda, S., 1990. Mechanism of back-arc opening in the Japan Sea: role of asthenospheric injection. Tectonophysics, 181, 299–306.

Wernicke, B. and Burchfiel, B.C., 1982, Modes of extensional tectonics. Journal of Structural Geology, 4, 105–115.

Wernicke, B., 1981, Low-angle normal faults in the Basin and Range province: nappe tectonics in an extending orogen. Nature, 291, 645–648.

White, N.J., Jackson, J.A. and McKenzie, D.P., 1986, The relationship between the geometry of normal faults and that of the sedimentary layers in their hangingwall. Journal of Structural Geology, 8, 897–909.

Wilcox, R.E., Harding, T.P. and Seely, D.R., 1973, Basic wrench tectonics. American Association of Petroleum Geologists Bulletin, 63, 2183–2191.

Wise, D.U., 1992, Dip domain method applied to the Mesozoic Connecticut Valley Rift Basins. Tectonics, 11, 1357–1368.

Yoon, S.H. and Chough, S.K., 1995, Regional strike slip in the eastern continental margin of Korea and its tectonic implications for the evolution of Ulleung Basin, East Sea (Sea of Japan). Geological Society of America Bulletin, 107, 83–97.

Yoon, S., 1976, The geological and paleontological study of the Tertiary deposits of the Janggi–Eoil district of Korea. No. 1. Stratigraphy and geologic age of the Songjeon Formation. Journal of Science, Pusan National University, 15, 67–71.

Yoon, S., 1982, Tertiary stratigraphy of the Eoil Basin, Korea. Journal of Geological Society of Korea, 18, 173–180.

Yun, H., Paik, K.-H. and Chang, S.K., 1989, Paleoecology of the Eoil Basin based on the organic and calcareous microfossils. Journal of the Paleontological Society of Korea, 5, 65–90.

Manuscript received February 12, 1999
Manuscript accepted July 15, 2000